

## Critical behavior in $\text{LaTiO}_{3+\delta/2}$ in the vicinity of antiferromagnetic instability

Y. Taguchi

*Department of Applied Physics, University of Tokyo, Tokyo 113-8656, Japan*

T. Okuda

*Joint Research Center for Atom Technology, Tsukuba 305-0046, Japan*

M. Ohashi, C. Murayama, N. Mōri, and Y. Iye

*Institute for Solid State Physics, University of Tokyo, Tokyo 106-8666, Japan*

Y. Tokura

*Department of Applied Physics, University of Tokyo, Tokyo 113-8656, Japan  
and Joint Research Center for Atom Technology, Tsukuba 305-0046, Japan*

(Received 18 September 1998)

The critical behavior in the vicinity of antiferromagnetic instability has been investigated for the filling-controlled insulator-metal transition system,  $\text{LaTiO}_{3+\delta/2}$ , by transport and specific heat measurements. With the increase of nominal hole doping  $\delta$ , the system undergoes a phase change from an insulating phase to a metallic phase at  $\delta_c^{\text{IM}} \approx 0.05$  and the low-temperature antiferromagnetic phase disappears at  $\delta_c^{\text{mag}} \approx 0.08$ . The Hall coefficient for an antiferromagnetic metallic crystal of  $\delta \approx 0.06$  shows a broad minimum near the Néel temperature while that for the compound of  $\delta = \delta_c^{\text{mag}}$  exhibits little temperature variation. At the antiferromagnetic instability point, the electronic specific heat coefficient  $\gamma$  as well as the coefficient  $\beta$  of  $T^3$  term of specific heat takes a maximum value as a function of  $\delta$ . High-pressure measurements of resistivity and Hall coefficient revealed that not only the antiferromagnetic spin correlation but also randomness effect plays an important role in producing an unconventional metallic state in the immediate vicinity of the magnetic instability point of the present compound. [S0163-1829(99)00112-5]

### I. INTRODUCTION

Recent extensive investigations on anomalous metallic states derived from Mott insulators have shed light on generic features of the highly correlated electron system and led to the discovery of versatile intriguing phenomena.<sup>1</sup> One way to obtain a metallic state from Mott insulators is to enhance one-electron transfer interaction, and hence to reduce relative strength of electron correlation effect with application of an external pressure, such as done in  $\text{V}_2\text{O}_3$  (Ref. 2) and  $\text{PrNiO}_3$ ,<sup>3</sup> or with modification of chemical composition, as employed in  $R\text{NiO}_3$  ( $R$  being a rare earth ion)<sup>4</sup> and  $\text{Ni}(\text{S},\text{Se})_2$ .<sup>5</sup> In addition to such a bandwidth-controlled insulator-metal transition at a constant (integer) band-filling, another successful way of driving an insulator-metal transition is to vary the electron filling from integer (filling-controlled insulator-metal transition). This has extensively been applied to various transition metal oxides, in particular, in this decade after the discovery of high- $T_c$  superconductivity in filling-controlled cuprate compounds. In filling-controlled insulator-metal transitions, many unconventional phenomena have been unraveled, for instance, charge-ordering transition in a stripe form,<sup>6</sup> incommensurate spin density wave transition with strong carrier-mass renormalization,<sup>7,8</sup> colossal magnetoresistance,<sup>9</sup> and so on. Among them, a perovskite-type titanate system  $\text{La}_{1-x}\text{Sr}_x\text{TiO}_{3+y/2}$  is known to be a canonical system for the filling-controlled insulator-metal transition and has widely been studied by transport,<sup>10-12</sup> thermodynamic,<sup>13</sup> and spectroscopic measurements,<sup>14-16</sup> as well as theoretically.<sup>17,18</sup>

One of the advantages in studying this particular class of

titanate lies in its relatively simple electronic and lattice features; namely, in a stoichiometric compound  $\text{LaTiO}_3$  a relevant electron is only single  $3d$  electron per each Ti site, whose network forms a simple, approximately cubic, lattice. The stoichiometric compound is a Mott-Hubbard type insulator with a charge gap of ca. 0.2 eV,<sup>16</sup> not a charge-transfer type insulator,<sup>19</sup> and hence the oxygen electronic states do not have to be taken into account explicitly as a first approximation. A magnetic transition takes place at around 140 K from a high-temperature paramagnetic phase to a low-temperature antiferromagnetic phase with minute spin canting ( $< 1^\circ$ ). With substituting La site by  $\text{Sr}(x)$  and/or introducing excess oxygen ( $y/2$ ), we can dope  $\delta$  ( $=x+y$ ) holes per Ti site and hence control the band filling ( $n=1-\delta$ ). As the doping  $\delta$  proceeds from 0 to 0.1, Néel temperature ( $T_N$ ) goes down and the antiferromagnetic long-range order disappears<sup>12</sup> (see also Fig. 3). For the sufficiently hole-doped metallic regime with  $\delta \geq 0.1$ , low-energy physics is basically understood in terms of conventional Landau-Fermi-liquid theory with renormalization of carrier effective mass in a strongly filling-dependent manner.<sup>11,13,17,18</sup> Many of the characteristic fingerprints for Fermi liquid, such as  $T$ -squared resistivity,  $T$ -independent Pauli-like susceptibility, and  $T$ -linear electronic specific heat are observed, and carrier effective mass is critically enhanced as the insulator-metal phase change is approached from the metallic side, reflecting the dominance of electron correlation effect associated with the metal-insulator transition. Optical measurements have also captured such a strong correlation effect over a higher energy scale of 1 eV order.<sup>14-16</sup> Overall features of the insulator-metal transition have so far been unraveled as men-

tioned above, yet the nature of critical regime between the stoichiometric insulating compound and heavily doped metallic phase is left to be explored in light of quantum critical phenomena in the course of the Mott transition. Here we note that there exist two quantum phase transitions on the way from the Mott insulator to the Fermi liquid; one is an antiferromagnetic-paramagnetic transition, the other is an insulator-metal transition. We have a possibility to find out, just at the magnetic phase transition, such a non-Fermi-liquid behavior as observed in a heavy fermion system<sup>20</sup> and also expected from a renormalization group analysis.<sup>21</sup> In the vicinity of the insulator-metal transition, which takes place away from integer filling, some effects other than electron correlation, in particular, Anderson localization, are also expected to play a role. Such a Mott-Anderson transition in correlated electron systems is a subject of recent vital theoretical studies<sup>22,23</sup> and should be experimentally clarified in a systematic way. If the two transitions occur at similar doping levels, and this is indeed the case in the present system (*vide infra*), complex but intriguing phenomena are likely to be observed at the critical region. In order to clarify such a critical region, we have made transport and thermodynamic measurements on the crystals whose hole concentration  $\delta$  is finely tuned near the insulator-metal transition point ( $\delta_c^{\text{IM}} \approx 0.05$ ) and the magnetic instability point ( $\delta_c^{\text{mag}} \approx 0.08$ ). In this paper, the fine control of the doping level  $\delta$  or the band filling ( $n = 1 - \delta$ ) was executed by introducing excess oxygen (i.e.,  $\delta = y$  and  $x = 0$ ), as was previously performed in another prototypical Mott transition system  $\text{V}_2\text{O}_3$ .<sup>24,25</sup> The filling control alone, in reality, cannot be made finely enough by its chemical nature to reveal all the critical behaviors of interest. Therefore, in addition to the filling control, we have utilized a high-pressure technique for a finer tuning as is often employed in heavy fermion systems.<sup>20</sup> External pressure causes an increase of the one-electron bandwidth or equivalently a reduction in the relative strength of the electron correlation effect, which enables us to probe the critical behavior in more detail.

## II. EXPERIMENT

All the crystals investigated here were grown by the floating zone method. We prepared the sample with different  $\delta$  by changing the atmosphere ( $\text{H}_2/\text{Ar}$  mixture 0–7%) as well as the feeding speed (5–20 mm/h) during the crystal growth. The excess oxygen content  $\delta/2$  could be accurately determined by the thermogravimetric analysis.<sup>26</sup> Resistivity measurements were carried out by a conventional four-probe method, using indium as an electrode. Magnetization measurements were done for the same samples as used in resistivity measurements, which are typically of  $3 \times 1 \times 1 \text{ mm}^3$  in size and of 10 mg in weight. The Hall coefficient was measured by rotating samples in a constant magnetic field of 5 T (7 T) for  $\delta \approx 0.01$  and 0.04 (for  $\delta \approx 0.06, 0.08$ , and 0.16) and fitting the Hall voltage with a sinusoidal curve at several temperatures. We have measured specific heat by a conventional relaxation method down to 0.5 K. Temperature variation of resistivity of the crystals with  $\delta \approx 0.06$  and 0.08 under high pressures up to 2.0 GPa was measured in a tungsten-carbide piston-cylinder apparatus, and the pressure was kept constant during a temperature sweep using a

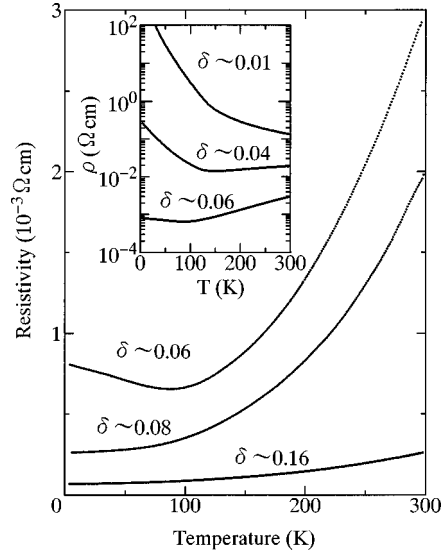


FIG. 1. Temperature variation of resistivity for metallic crystals. Inset shows the resistivity for insulating compounds on a logarithmic scale. The sample of  $\delta \approx 0.06$  is included for comparison.

constant-load generating system.<sup>27</sup> We also measured the Hall coefficient at 4.2 K under high pressures by a conventional six-terminal method. Hall voltage ( $V_H$ ) was monitored with the change of the magnetic field ( $B$ ) up to  $\pm 5$  T and the Hall coefficient was estimated from the slope of the  $V_H$ - $B$  line.

## III. DOPING DEPENDENCE OF TRANSPORT AND SPECIFIC HEAT PROPERTIES NEAR THE CRITICAL POINT

In Fig. 1 we display the temperature dependence of the resistivity for samples with several doping concentrations, ranging from 0.01 to 0.16. As shown in the inset, the sample with  $\delta \approx 0.01$  shows an insulating behavior below room temperature. The resistivity for the  $\delta \approx 0.04$  crystal exhibits an upturn at around 130 K and increases with further lowering temperature. In the main panel of Fig. 1 is shown resistivity of the compound whose ground state is metallic (the compound of  $\delta \approx 0.06$  is exemplified also in the inset to show a difference from the insulating samples). The crystal with  $\delta \approx 0.06$  also shows an upturn at around 90 K (slightly below  $T_N$ ), but the resistivity remains finite even at the lowest temperature. The resistivity of the  $\delta \approx 0.08$  crystal continues to decrease down to the lowest temperature. It is worth noting that the resistivity for  $\delta \approx 0.06$  and 0.08 well exceeds the Mott limit ( $\approx 0.5 \text{ m}\Omega \text{ cm}$  in the present case) in a certain range of temperature, and hence these two crystals should be called a “bad metal” according to the nomenclature by Emery and Kivelson.<sup>28</sup> The sample of  $\delta \approx 0.16$  shows a qualitatively different behavior from the other two metallic samples: residual resistivity is less than  $100 \mu\Omega \text{ cm}$  and a rapid increase above 100 K seen in the former two samples is absent.

We show in Fig. 2 the temperature dependence of magnetization under a magnetic field of 100 Oe. As we mentioned before, the antiferromagnetic spin ordering accompa-

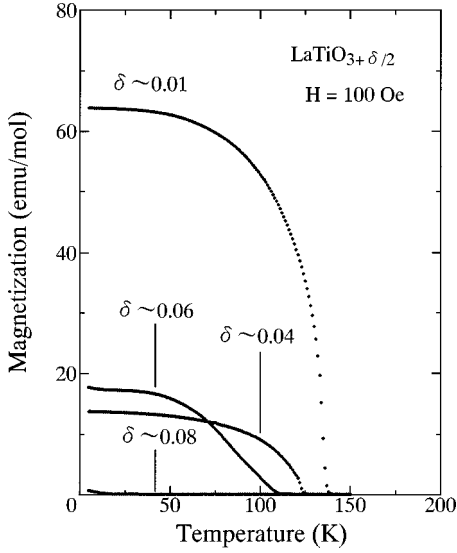


FIG. 2. Temperature dependence of magnetization under a magnetic field of 100 Oe.

nies a minute amount of spin canting. Therefore, we can unambiguously determine the Néel temperature for each crystal by the onset of the magnetization. As the doping concentration is increased, the Néel temperature is reduced from about 140 K, and is likely to disappear at a doping concentration of  $\delta \approx 0.08$ .

We summarize the results of resistivity and magnetization measurements in Figs. 3(a) and 3(b) as a function of doping level  $\delta$ , together with those of the Hall coefficient in Fig. 3(c) and the specific heat in Figs. 3(d) and 3(e). As shown in Fig. 3(a), the  $T \rightarrow 0$  conductivity  $\sigma_0$  (inverse of residual resistivity) is negligible for  $\delta < 0.05$  and the ground state is an insulator, while  $\sigma_0$  for  $\delta \geq 0.06$  is finite and a metallic ground state is realized. The filling-controlled insulator-metal transition occurs at the critical hole concentration of  $\delta_c^{\text{IM}} \approx 0.05$ . The  $\sigma_0$  for  $\delta > 0.05$  seems to increase approximately linearly with the change of  $\delta$ , which is often observed in the Mott-Anderson transition system.<sup>29</sup> We show in Fig. 3(b) the magnetic transition temperature ( $T_N$ ) and the magnetization under 100 Oe at 5 K. As holes are doped into the system, it is likely (provided that the canting angle is unchanged) that the net moment shrinks eventually to disappear at critical doping concentration  $\delta_c^{\text{mag}} \approx 0.08$ , which is slightly larger than  $\delta_c^{\text{IM}} (\approx 0.05)$ . From the results of Figs. 3(a) and 3(b), the ground state of the system is an antiferromagnetic insulator for  $\delta < 0.05$ , *antiferromagnetic metal* for  $\delta = 0.06 - 0.08$ , and paramagnetic metal for  $\delta > 0.08$ .

We plot in Fig. 4 the temperature variation of the Hall coefficient ( $R_H$ ). All the values are of minus sign, indicating electronlike charge carriers in agreement with the previous result for  $\delta \geq 0.1$ .<sup>11</sup> The  $R_H$  of insulating compounds of  $\delta \approx 0.01$  and 0.04 show strong temperature dependence, and are likely to diverge with lowering temperature, although they cannot be measured below 120 K (100 K) for  $\delta \approx 0.01$  (0.04) because of too low mobility. On the other hand, the  $R_H$  of metallic crystals ( $\delta \approx 0.06, 0.08$ , and 0.16) show a relatively weak temperature variation, compared with the insulating compounds. A density of one carrier per Ti site gives the  $R_H$  value of  $0.4 \times 10^{-3} \text{ cm}^3/\text{C}$  according to a

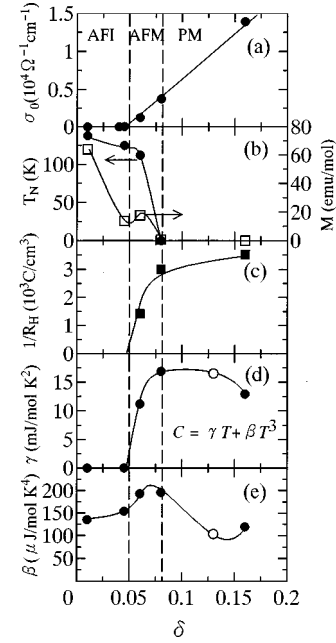


FIG. 3. (a) Conductivity ( $\sigma_0$ ) in  $T \rightarrow 0$  limit, (b) antiferromagnetic spin-ordering temperature ( $T_N$ ) and spontaneous magnetization ( $M$ , taken at 5 K under 100 Oe) due to minute canting of the antiferromagnetically ordered spin, (c) inverse of Hall coefficient ( $R_H$ ) at 2 K (d) electronic specific heat coefficient ( $\gamma$ ), and (e) coefficient of  $T^3$  term of specific heat ( $\beta$ ), as a function of hole concentration  $\delta$ . Vertical dashed lines denote the insulator-metal ( $\delta_c^{\text{IM}} \approx 0.05$ ) and antiferromagnetic-paramagnetic ( $\delta_c^{\text{mag}} \approx 0.08$ ) phase boundaries. Solid lines are the guides to the eyes. Open symbols in (d) and (e) are the results for  $\text{La}_{0.95}\text{Sr}_{0.05}\text{TiO}_{3.04}$  reproduced from Ref. 13. AFI, AFM, and PM stand for antiferromagnetic insulator, antiferromagnetic metal, and paramagnetic metal, respectively.

simple Drude model of  $R_H = 1/ne$ , where  $n$  is carrier density and  $e$  is electron charge. Although in a real material quantitative analysis of  $R_H$  should be made with a real band structure, small Hall coefficients certainly indicate that the crys-

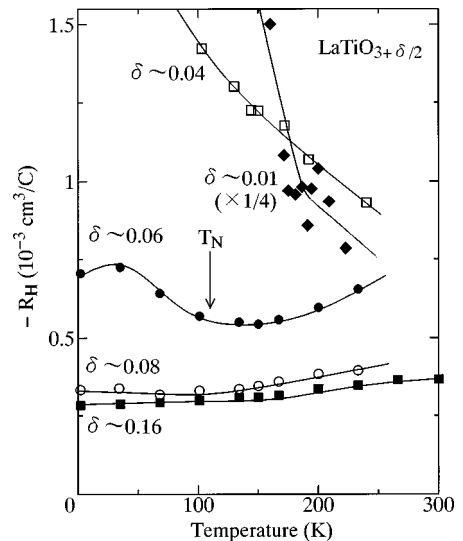


FIG. 4. Temperature variation of Hall coefficient ( $R_H$ ). The  $R_H$  is negative for all the samples. The data points for  $\delta \approx 0.01$  are multiplied by a factor of  $\frac{1}{4}$ . Solid lines are the guides to the eyes.

tals of  $\delta \approx 0.08$  and  $0.16$  have a large Fermi surface, consistent with the band filling  $1 - \delta$ . The  $R_H$  of the  $\delta \approx 0.06$  sample is about two times as large as those of  $\delta \approx 0.08$  and  $0.16$  at the lowest temperature, which can be attributed to an opening of the spin-density wave (SDW) gap over about half of the original Fermi surface area. This will be clearly evidenced by the pressure effect on  $R_H$  as described in the next section. Thus, the crystal of  $\delta \approx 0.06$  without SDW would also show a large Fermi surface corresponding to an electron density of  $1 - \delta$ . The lowest-temperature ( $2\text{ K}$ ) value of  $R_H^{-1}$  is plotted in Fig. 3(c) as a measure of carrier density in the ground state.

Let us focus our attention on the temperature dependence of  $R_H$  for  $\delta \approx 0.06$ . Two factors are likely to be responsible for the observed temperature dependence. First, one is a thermally induced increase of the effective carrier number or equivalently restoration of the original Fermi surface area, which should lead to a reduction of  $R_H$ , as the temperature is increased from the lowest temperature toward  $T_N$ . Another factor originates from a thermally induced crossover in nature of charge carriers from low-temperature electronlike carriers with a large Fermi surface to high-temperature holelike carriers characteristic of a hole pocket. Recently, temperature variation of frequency-dependent  $R_H$  in hole-doped Mott insulators in two-dimension (2D) has been studied numerically,<sup>30</sup> and shown to cross over from electronlike  $R_H$  at  $T < J$  ( $= 4t^2/U$ ) to holelike one at  $J < T < U$ . In a language of dynamical mean-field theory,<sup>18</sup> low-temperature transport is dominated by quasiparticles with a large Fermi surface satisfying the Luttinger theorem, and hence a negative small value of  $R_H$  should be observed. On the other hand, at high temperatures, where Kondo resonance or coherence peak in the single-particle spectral function is absent, a rigid band picture of Hubbard gives an accurate description of physics, and therefore a large positive value of  $R_H$  is expected.<sup>18</sup> In view of the close proximity of this crystal to the insulator-metal transition point ( $\delta^{\text{SM}} \approx 0.05$ ), such a crossover is likely to occur, which leads to an enhancement of  $R_H$ , as the temperature is increased from the lowest temperature. These two factors may yield the observed temperature variation of  $R_H$ , namely, a broad minimum near  $T_N$ .

The crystal of  $\delta \approx 0.08$  shows a very weak temperature dependence, which rather mimics that of  $\delta \approx 0.16$ , locating deep in the paramagnetic phase. Such a seemingly normal behavior of  $R_H$  even at the magnetic instability point is contrasted by an anomalous feature of  $R_H$  observed and theoretically conjectured for a 2D case. Recently, a ‘‘Fermi-surface segment’’ was observed by angle-resolved photoemission experiments near  $(\pi/2, \pi/2)$  point in  $k$  space in underdoped high- $T_c$  cuprate superconductors.<sup>31,32</sup> In relevance to these experiments, the mean-field phase diagram as a function of doping was studied theoretically<sup>33</sup> with  $SU(2)$  formulation of the  $t$ - $J$  model, and it was shown that the Fermi surface shape evolves from a segment near the  $(\pi/2, \pi/2)$  point in an underdoped region just next to the antiferromagnetic phase toward a full Fermi surface satisfying the Luttinger theorem at a higher doping level. If such a Fermi surface segment were of a generic feature among compounds in the vicinity of the antiferromagnetic phase, an enhancement of  $R_H$  due to a shrinkage of the Fermi surface might be observed as the antiferromagnetic spin correlation is enhanced with the de-

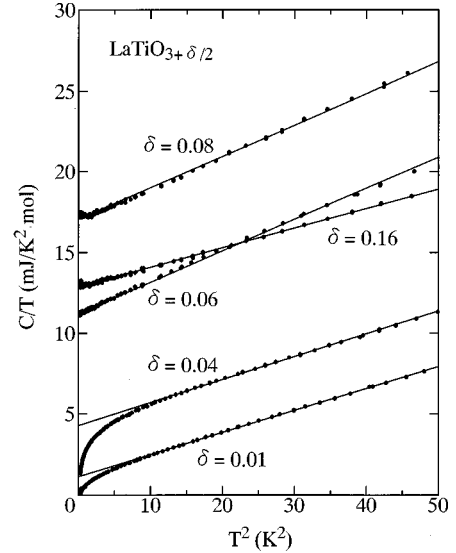


FIG. 5. Low-temperature specific heat ( $C$ ) plotted in a form of  $C/T$  versus  $T^2$ . Solid lines are fitted lines with a formula of  $C/T = \gamma + \beta T^2$  in a temperature range of  $10\text{ K}^2 \leq T^2 \leq 50\text{ K}^2$  for  $\delta \approx 0.01$  and  $0.04$ , and of  $T^2 \leq 50\text{ K}^2$  for  $\delta \approx 0.06, 0.08$ , and  $0.16$ .

crease of temperature toward the magnetic quantum critical point. As will be shown later, in this specific compound of  $\delta \approx 0.08$ , an antiferromagnetic spin correlation is likely to develop sufficiently at low temperatures in view of an enhanced  $T^3$  term of specific heat. Nevertheless, such an increase of  $R_H$  cannot be observed even in the present crystal just at the magnetic instability point. The absence of the increase of  $R_H$  even in the immediate vicinity of the antiferromagnetic-paramagnetic and/or insulator-metal transition point may be attributed to a difference in electronic dimension (2D vs 3D) of the cuprates and the present titanates.

In Fig. 5, we show the result of specific heat measurements, in a form of  $C/T$  vs  $T^2$ . With decreasing the doping level from  $\delta \approx 0.16$  to  $\delta \approx 0.08$ ,  $\gamma$  and  $\beta$  are both enhanced, where  $\gamma$  (intersection) and  $\beta$  (slope) are defined as  $C/T = \gamma + \beta T^2$ . [See also Figs. 3(c) and 3(d).] Further reducing the doping level below  $0.08$  leads to a reduction of the  $\gamma$  value as well as of the slope  $\beta$ . For the samples with  $\delta \approx 0.01$  and  $0.04$ ,  $C/T$  begins to decrease below  $T^2 < 10\text{ K}^2$  toward zero. In a heavy fermion system,<sup>20</sup> dramatic deviation from constant  $\gamma$  value at low temperatures is observed just at the magnetic instability point. In the present system, the crystal of  $\delta \approx 0.08$ , just at the magnetic critical point, shows a very slight upturn at about  $1.2\text{ K}$  (barely discernible in the present scale of Fig. 5). If we assume this upturn is due to a critical spin fluctuation and fit the data with the renormalization group theory by Millis *et al.*<sup>21</sup> we obtain a coherence temperature of  $270\text{ K}$  (referred to as  $T^*$  in Ref. 21), which should be of the order of Fermi temperature. On the other hand, the Sommerferd constant  $\gamma$  of this compound,  $\approx 17\text{ mJ/mol K}^2$ , yields a Fermi temperature of  $2400\text{ K}$ , which is one order of magnitude larger than that derived from the fitting procedure. Therefore, we cannot fit the data quantitatively with the renormalization group theory. The absence of a significant temperature dependence of  $\gamma$  is perhaps due to a fairly high-degenerate temperature in this

3*d*-electron system, presumably two orders of magnitude larger than that of the *f*-electron system.

In Fig. 3(d),  $\gamma$  values are plotted against the doping rate  $\delta$ . As the antiferromagnetically spin-ordered phase is approached from the paramagnetic side,  $\gamma$  is enhanced due to a strong electron-correlation effect,<sup>11</sup> takes a maximum value ( $\approx 17$  mJ/mol K<sup>2</sup>) at the magnetic instability point  $\delta_c^{\text{mag}}$ , and is followed by a reduction in the antiferromagnetic metallic phase. Such dependence of  $\gamma$  on the control parameter is observed in other systems, for example,  $\text{NiS}_{2-x}\text{Se}_x$ ,<sup>34</sup> in which the parameter is the one-electron bandwidth as opposed to the band filling in the present case. Another example for the enhanced Sommerferd constant  $\gamma$  in the antiferromagnetic metallic phase is for the filling-controlled system  $\text{V}_{2-y}\text{O}_3$ ,<sup>35</sup> where  $\gamma$  increases with the decrease of  $T_N$  but a paramagnetic ground state cannot be achieved by filling control alone. All these cases including the present system can be qualitatively understood as follows. At the critical parameter value, the spin correlation length diverges toward absolute zero temperature and the characteristic energy of the spin fluctuation decreases faster than temperature, and hence low-lying spin fluctuation persists down to  $T=0$  and contribute to the specific heat. As the compound enters into the antiferromagnetic phase, some portion of the Fermi surface is gapped and the density of states at the Fermi level decreases. This was also confirmed by preliminary results of a photoemission experiment<sup>36</sup> on the  $\delta \approx 0.06$  crystal. On the other hand, as the compound goes away from the critical point in the paramagnetic phase, the less important the electron correlation effect is, and consequently the less  $\gamma$  is enhanced.

The decrease of  $\delta$  below 0.05 drives the system insulating, but the apparent  $\gamma$  value, which is extrapolated from the points of  $10 \text{ K}^2 \leq T^2 \leq 50 \text{ K}^2$  to  $T=0$  has nonzero values for  $\delta=0.04$  and 0.01, although the value of  $C/T$  decreases steeply toward zero below  $T^2 \leq 10 \text{ K}^2$  for the both samples. The result implies that a finite density of states is present very near the Fermi level but that a minimal gap of about 3 K opens just at the Fermi level. This might signal that the insulator-metal transition in this system is influenced by an Anderson localization effect, although the strong electron-correlation effect does play an important role in preparing the strongly mass-renormalized state that is amenable to the Anderson localization.

In Fig. 3(e), the coefficient  $\beta$  of the  $T^3$  term is plotted as a function of hole concentration  $\delta$ . As is well known, the contribution from a three-dimensional antiferromagnetic spin wave to specific heat is proportional to  $T^3$ . Therefore, the  $\beta$  value in the antiferromagnetic phase ( $\delta < 0.08$ ) contains contributions from both phonons and magnons. One may notice that the  $\beta$  value as well as  $\gamma$  takes a maximum at the magnetic instability point and is reduced either in the paramagnetic metallic side or in the antiferromagnetic insulating side. Such an enhancement of the  $T^3$  term toward the magnetic critical point basically originates from increasing magnon contribution due to a critical softening of spin stiffness even though spin wave excitations are not well-defined modes at the critical point. The amount of such an enhancement, however, seems to be too large to be attributed only to magnon contribution, as in the light of the following quantitative estimate: the Heisenberg spin model in a 3D cubic lattice pre-

dicts that the nearest-neighbor exchange constant  $J$  would be about 6 meV when  $T_N$  is 140 K, which makes a contribution to the  $\beta$  value by an amount as small as  $12 \mu\text{J/mol K}^4$ . Therefore, 91% of the  $\beta$  value in  $\delta \approx 0.01$  comes from other degrees of freedom than the spin wave, such as lattice vibration. As for the sample of  $\delta \approx 0.16$ , contribution from magnetic excitation is likely to be also small because it is deep in the metallic phase. Provided that the phonon contribution to the  $\beta$  is roughly of  $120 \mu\text{J/mol K}^4$ , which should be as large as the  $\beta$  values for  $\delta \approx 0.01$  and 0.16, over the whole doping range considered here, in the samples with  $\delta \approx 0.06$  and 0.08, about  $70 \mu\text{J/mol K}^4$  comes from magnon or other related low-lying excitation. Here we adopt a metallic antiferromagnetic model,<sup>37</sup> in which the spin-wave dispersion is given by  $\omega_k = \frac{1}{3}v_F k$  for the small value of  $k$ , where  $v_F$  is Fermi velocity. If we assume only the spin-wave contribution is responsible for all of the additional  $70 \mu\text{J/mol K}^4$ , we obtain Fermi velocity of  $v_F = 2.1 \times 10^6$  cm/s, which results in the carrier effective mass of  $m^*/m_0 \sim 42$ ,  $m_0$  being free electron mass. This value is within an acceptable range of magnitude, but is somewhat large, compared with the value  $m^*/m_0 \sim 11$ , estimated from the observed Sommerferd constant  $\gamma$ . This implies a possibility that there exists another type of bosonic excitations, which contribute to the specific heat. In the present compound, the relevant electron is accommodated to the triply degenerated  $t_{2g}$  orbital, and hence has an orbital degree of freedom. Orbital ordering and orbital wave excitation are recently discussed in many transition metal oxides, in particular, perovskite-type manganites and its layered compounds.<sup>38,39</sup> It is reasonable to anticipate that such an orbital ordering also takes place in the present antiferromagnetic compounds, although there has been thus far no direct evidence in this system. Therefore, softened orbital waves may make some contribution to the  $\beta$  value, especially in the vicinity of the magnetic critical point near which the orbital ordering is also likely to disappear.

#### IV. PRESSURE DEPENDENCE OF TRANSPORT PROPERTIES NEAR THE CRITICAL POINT

Since the tuning by filling control is discrete by nature, we have tried to investigate the critical region in more detail with use of high pressure. The role of pseudohydrostatic pressure is to enhance the electron hopping and hence to decrease the electron correlation strength.<sup>1,12</sup> We have performed high-pressure experiments for two particular compounds. One is  $\delta \approx 0.06$ , which is an antiferromagnetic metal, and the other is  $\delta \approx 0.08$ , which is just at the magnetic instability point (see Fig. 3). We show in Fig. 6(a) temperature dependence of resistivity for  $\delta \approx 0.06$  under various pressures. At ambient pressure, this sample undergoes a transition to the antiferromagnetic state at  $T_N = 112$  K. Resistivity under the atmospheric pressure decreases quite steeply below 300 K with lowering the temperature, takes the minimum at a slightly lower temperature than  $T_N$ , which we define as  $T^*$ , and then gradually increases. In a temperature range below  $T^*$ , the temperature derivative of resistivity is negative. However, the resistivity shows saturation and remains finite down to 40 mK (not shown here), indicating a metallic ground state. The negative temperature derivative of resistivity only means that the effective carrier number is getting

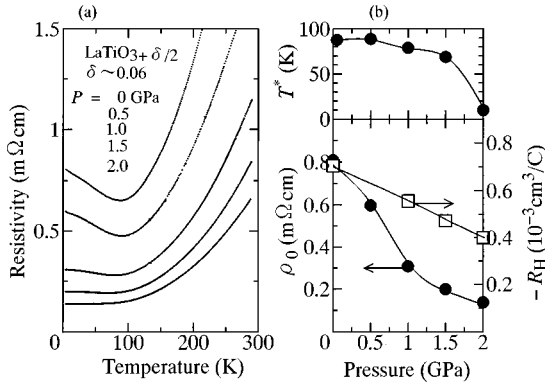


FIG. 6. (a) Temperature variation of resistivity for  $\delta \approx 0.06$  under various applied pressures. (b) Pressure dependence of temperature of resistivity minimum  $T^*$  (upper panel), residual resistivity  $\rho_0$  (closed circles, lower panel), and Hall coefficient  $R_H$  at 4.2 K (open squares, lower panel). Solid lines in (b) are the guides to the eyes.

smaller due to a gradual opening of the SDW gap over some portion of the Fermi surface as the temperature is decreased, and does not mean emergence of an insulating state, which should correspond to a complete opening of a gap over the whole Fermi surface area or equivalently a complete destruction of the Fermi surface. Such a negative temperature derivative of resistivity below  $T_N$  is also observed in another SDW transition system,  $V_{2-y}O_3$ , and has been similarly interpreted as a *metallic* antiferromagnet.<sup>7</sup> The resistivity value of the  $\delta \approx 0.06$  crystal at ambient pressure is higher than the characteristic Mott limit ( $\approx 0.5$  m $\Omega$  cm) over the whole temperature range and the steep increase above  $\approx 100$  K is reminiscent of the thermally induced coherent-incoherent crossover, which is generic for a correlated metal,<sup>2,40</sup> as predicted by the dynamical mean-field theory.<sup>41</sup> With the application of pressure, we observed a huge reduction in resistivity, both in residual resistivity and high-temperature resistivity.

We show  $T^*$  in the upper panel of Fig. 6(b) as a function of applied pressure. Although the important quantity under an external pressure is the Néel temperature, we cannot determine it from this resistivity data because of the least anomaly in the resistivity at the magnetic transition temperature (at ambient pressure) apart from a gentle upturn below  $T^*$ . Therefore, we plot  $T^*$  instead of  $T_N$ , since these temperatures are more or less correlated. Resistivity upturn is robust against pressure, and  $T^*$  shows little change against pressures less than 1.5 GPa. Applying a pressure of 2 GPa, however, the resistivity upturn can be almost suppressed. We can infer that the antiferromagnetic ordering is accordingly suppressed in the pressurized sample, but cannot conclude from these transport data alone the perfect change into the paramagnetic state at high pressures, say  $> 1.5$  GPa.

In the lower panel of Fig. 6(b) is plotted the residual resistivity ( $\rho_0$ ) as well as the Hall coefficient ( $R_H$ ) at 4.2 K (viewed as representing the ground state) as a function of applied pressure. The  $\rho_0$  and  $R_H$  are reduced by a factor of 1/6 and 1/2, respectively, under the pressure of 2 GPa. Such a large variation in  $\rho_0$  and  $R_H$  is interpreted in terms of pressure-suppression of the SDW state. Residual resistivity

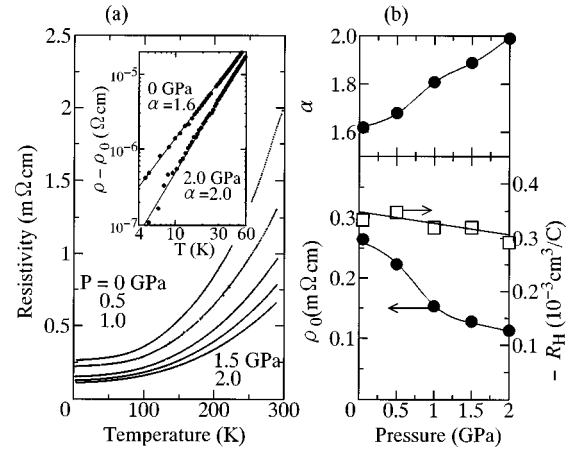


FIG. 7. (a) Temperature dependence of resistivity for  $\delta \approx 0.08$  under various applied pressures. The inset to (a) exemplifies  $T^\alpha$ -type dependence of resistivity below 60 K at ambient pressure and 2.0 GPa, and straight lines correspond to  $\alpha = 1.6$  and 2.0 dependencies, respectively. (b) Pressure dependence of residual resistivity  $\rho_0$  (closed circles, lower panel), Hall coefficient  $R_H$  at 4.2 K (open squares, lower panel), and the power  $\alpha$  (upper panel) defined as  $\rho = \rho_0 + AT^\alpha$ . Solid lines in (b) are merely the guides to the eyes.

is given<sup>42</sup> by  $\rho_0 = 12\pi^3\hbar/e^2 1/S_F l$ , where  $S_F$  is the area of the Fermi surface, and  $l$  the mean free path for elastic scattering. The Hall coefficient is expressed<sup>43</sup> as  $R_H = (12\pi^3/ec)(1/k_F/S_F)$ , where  $1/k_F$  is the average curvature of the Fermi surface. Therefore, the both quantities<sup>42,43</sup> are a good measure for the Fermi surface area. At ambient pressure, the SDW gap opens up below  $T_N$  over some region of the Fermi surface, which causes the reduction of the Fermi surface area or effective carrier number and the concomitant increase of resistivity. With the application of pressure, we apparently drive the system toward the paramagnetic phase and suppress the SDW state via the pressure-induced increment of the one-electron bandwidth. Therefore, the lost area of the Fermi surface is partly restored under high pressure, which results in the reduction of both residual resistivity and the Hall coefficient. The difference in the magnitudes of the pressure-induced reduction in  $\rho_0$  and  $R_H$  may be attributed to their different response to the localization effect, which more clearly emerges in the case of  $\delta \approx 0.08$ , as detailed below.

Figure 7 is concerned about the high-pressure study for the  $\delta \approx 0.08$  crystal, which locates just at the magnetic instability point. This sample shows neither spontaneous magnetization nor resistivity upturn down to 4.2 K. Resistivity under pressure is displayed in Fig. 7(a). At ambient pressure, the temperature dependence of resistivity changes at around 70 K;  $\sim T^{1.6}$  at lower temperatures and  $\sim T^{2.5}$  at higher temperatures. Application of pressure largely reduces the resistivity also in this crystal, in particular the residual resistivity ( $\rho_0$ ). We show in the lower panel of Fig. 7(b) the pressure variation of  $\rho_0$  and  $R_H$  at 4.2 K. While the  $\rho_0$  decreases by a factor of 1/2 under 2 GPa,  $R_H$  at 4.2 K is almost pressure independent, making a striking contrast to the case of  $\delta \approx 0.06$ , in which these two quantities are both significantly reduced.

The randomness effect, perhaps caused by the presence of excess oxygen, may play a crucial role in the different re-

sponses of  $\rho_0$  and  $R_H$  to external pressure. The Hall effect in the disordered electron system was investigated first by Fukuyama<sup>44</sup> and Altshuler *et al.*,<sup>45</sup> using the perturbation expansion technique, and later by Shapiro and Abrahams,<sup>46</sup> using a scaling theory. These studies show that the Hall coefficient is unaffected by disorder as a first approximation and the conductivity can go to zero with the  $R_H$  unchanged. According to the scaling theory,<sup>46</sup> conductivity and Hall conductivity are expected to vary as  $\sigma(E) \approx (E - E_c)^\mu$  and  $\sigma_H(E) \approx (E - E_c)^{2\mu}$ ,  $E_c$  being the mobility edge. Thus, the Hall coefficient  $R_H = \sigma_H / \sigma^2$  is constant. When we apply pressure to an Anderson insulator and drive the system metallic, the conductivity increases with the  $R_H$  unchanged. Our experimental result, namely the reduction of  $\rho_0$  while  $R_H$  is being kept constant, is therefore understood consistently in terms of pressure suppression of the weak localization effect.

Another feature to be noted is a gradual change in temperature dependence of resistivity below 50 K with the application of pressure. Below 50 K, resistivity is well fitted by the equation  $\rho = \rho_0 + AT^\alpha$ , as exemplified for the cases of 0 and 2.0 GPa in the inset to Fig. 7(a). We adopt 50 K as a high-temperature cutoff for the fitting since the resistivity starts to increase radically above 70 K due to the aforementioned coherent-incoherent crossover. The power  $\alpha$  is plotted against applied pressure in the upper panel of Fig. 7(b). The  $\alpha$  appears to vary *continuously* from  $\approx 1.6$  at ambient pressure to  $\approx 2.0$  under the pressure of 2.0 GPa. The power of 1.5 is predicted by the self-consistent renormalization (SCR) theory<sup>47,48</sup> for the compound at the antiferromagnetic instability point, and is actually reported for  $\text{NiS}_{2-x}\text{Se}_x$  with  $x \approx 1$ .<sup>35,49</sup> The power of 2 is, as well known, characteristic of the Fermi liquid, and is indeed observed in this titanium system with a sufficient doping concentration, say  $\delta > 0.1$ .<sup>11</sup> Thus, we have observed a crossover from an anomalous metal near the magnetic quantum critical point to a conventional Fermi liquid. The standard SCR theory taking account of the spin fluctuation effect alone predicts<sup>47</sup> that at a fixed value of the control parameter, a crossover occurs around a certain temperature from lower-temperature  $T^2$  dependence to higher-temperature  $T^{1.5}$  dependence, and that the crossover temperature itself increases as the control parameter is varied away from the critical point. Obviously, this is not the case of our experiment, which indicates that the other effect has to be considered. The alternative relevant factor is the randomness effect, which is proved to be important by the aforementioned argument of  $\rho_0$  and  $R_H$ . Recently, Dobrosavljević and Kotliar<sup>22</sup> have studied the Mott-Anderson transition using a dynamical mean-field theory, where a control parameter is the relative strength of random potential to one-electron bandwidth, and have found the

presence of a non-Fermi-liquid phase between an insulating phase and a Fermi-liquid phase. Explicit calculation of temperature dependence of resistivity is not shown there, but the present compound ( $\delta \approx 0.08$ ) might have traversed this type of non-Fermi-liquid phase as the one-electron bandwidth is increased or equivalently the relative strength of randomness effect is decreased with the increase of pressure.

## V. CONCLUSION

We have clarified the critical behavior in the  $\text{LaTiO}_{3+\delta/2}$  system in the vicinity of antiferromagnetic instability ( $\delta_c^{\text{mag}}$ ) by transport and thermodynamic measurements. While the Hall coefficient ( $R_H$ ) of the antiferromagnetic metallic sample with  $\delta \approx 0.06$  increases below  $T_N$  due to the decrease of the effective carrier number, that of the sample with  $\delta \approx 0.08$ , just at the magnetic instability point, shows little temperature variation. Electronic specific heat coefficient  $\gamma$  takes a maximum value ( $\approx 17$  mJ/mol·K<sup>2</sup>) at  $\delta_c^{\text{mag}} \approx 0.08$  and is reduced in the antiferromagnetically ordered phase ( $\delta < \delta_c^{\text{mag}}$ ). The coefficient of  $T^3$  term  $\beta$  of specific heat exhibits a remarkable enhancement as well at the magnetic critical point, which is attributed to softened spin-wave-like excitations, and also possibly to orbital excitations. Residual resistivity and the Hall coefficient at 4.2 K for the antiferromagnetic metallic state with  $\delta \approx 0.06$  are both reduced under high pressure, which we interpret as due to pressure-suppression of the SDW state and resultant restoration of the Fermi surface area. By contrast, the barely paramagnetic compound with  $\delta \approx 0.08$  close to  $\delta_c^{\text{mag}}$  shows little change in the Hall coefficient in response to pressure, whereas a large reduction in residual resistivity is observed. This result indicates the relevance of the randomness effect and a dominant role of pressure in suppression of the weak localization effect. At  $\delta \approx \delta_c^{\text{mag}}$ , we also observe a pressure-induced crossover in the temperature dependence ( $T^\alpha$ ) of the low-temperature ( $T < 50$  K) resistivity from  $\alpha \approx 1.6$  to  $\alpha \approx 2.0$ . This may signal the pressure-induced traverse from a non-Fermi liquid to a Fermi-liquid state.

## ACKNOWLEDGMENTS

We are grateful to H. Fukuyama, M. Imada, N. Nagaosa, and H. Takagi for fruitful discussions and to Y. Okada for his collaboration at an early stage of this paper. This paper was in part supported by a Grant-In-Aid from the Ministry of Education, Science and Culture, Japan and by the New Energy and Industrial Technology Development Organization (NEDO).

<sup>1</sup>For a review, M. Imada, A. Fujimori, and Y. Tokura, *Rev. Mod. Phys.* **70**, 1039 (1998).

<sup>2</sup>D.B. McWhan, J.P. Remeika, T.M. Rice, W.F. Brinkman, J.P. Maita, and A. Menth, *Phys. Rev. Lett.* **27**, 941 (1971); D.B.

McWhan, A. Menth, J.P. Remeika, W.F. Brinkman, and T.M. Rice, *Phys. Rev. B* **7**, 1920 (1973).

<sup>3</sup>P.C. Canfield, J.D. Thompson, S-W. Cheong, and L.W. Rupp, *Phys. Rev. B* **47**, 12 357 (1993).

- <sup>4</sup>J.B. Torrance, P. Lacorre, A.I. Nazzari, E.J. Ansaldo, and Ch. Niedermayer, *Phys. Rev. B* **45**, 8209 (1992).
- <sup>5</sup>J.A. Wilson and G.D. Pitt, *Philos. Mag.* **23**, 1297 (1971).
- <sup>6</sup>C.H. Chen, S-W. Cheong, and A.S. Cooper, *Phys. Rev. Lett.* **71**, 2461 (1993).
- <sup>7</sup>S.A. Carter, T.F. Rosenbaum, J.M. Honig, and J. Spalek, *Phys. Rev. Lett.* **67**, 3440 (1991).
- <sup>8</sup>W. Bao, C. Broholm, S.A. Carter, T.F. Rosenbaum, G. Aeppli, S.F. Trevino, P. Metcalf, J.M. Honig, and J. Spalek, *Phys. Rev. Lett.* **71**, 766 (1993).
- <sup>9</sup>A. Urushibara, Y. Moritomo, T. Arima, A. Asamitsu, G. Kido, and Y. Tokura, *Phys. Rev. B* **51**, 14 103 (1995), and references cited therein.
- <sup>10</sup>F. Lichtenberg, D. Widmer, J.G. Bednorz, T. Williams, and A. Reller, *Z. Phys. B* **82**, 211 (1991).
- <sup>11</sup>Y. Tokura, Y. Taguchi, Y. Okada, Y. Fujishima, T. Arima, K. Kumagai, and Y. Iye, *Phys. Rev. Lett.* **70**, 2126 (1993).
- <sup>12</sup>Y. Okada, T. Arima, Y. Tokura, C. Murayama, and N. Môri, *Phys. Rev. B* **48**, 9677 (1993).
- <sup>13</sup>K. Kumagai, T. Suzuki, Y. Taguchi, Y. Okada, Y. Fujishima, and Y. Tokura, *Phys. Rev. B* **48**, 7636 (1993).
- <sup>14</sup>Y. Fujishima, Y. Tokura, T. Arima, and S. Uchida, *Phys. Rev. B* **46**, 11 167 (1992).
- <sup>15</sup>D.A. Crandles, T. Timusk, J.D. Garrett, and J.E. Greedan, *Phys. Rev. B* **49**, 16 207 (1994).
- <sup>16</sup>Y. Okimoto, T. Katsufuji, Y. Okada, T. Arima, and Y. Tokura, *Phys. Rev. B* **51**, 9581 (1995).
- <sup>17</sup>M.J. Rozenberg, G. Kotliar, and X.Y. Zhang, *Phys. Rev. B* **49**, 10 181 (1994).
- <sup>18</sup>H. Kajueter, G. Kotliar, and G. Moeller, *Phys. Rev. B* **53**, 16 214 (1996).
- <sup>19</sup>J. Zaanen, G.A. Sawatzky, and J.W. Allen, *Phys. Rev. Lett.* **55**, 418 (1985).
- <sup>20</sup>H. von Löhneysen, *J. Phys.: Condens. Matter* **8**, 9689 (1996), and references cited therein.
- <sup>21</sup>A.J. Millis, *Phys. Rev. B* **48**, 7183 (1993); U. Zülicke and A.J. Millis, *ibid.* **51**, 8996 (1995).
- <sup>22</sup>V. Dobrosavljević and G. Kotliar, *Phys. Rev. Lett.* **78**, 3943 (1997).
- <sup>23</sup>T.R. Kirkpatrick and D. Belitz, *Phys. Rev. Lett.* **73**, 862 (1994); **74**, 1178 (1995).
- <sup>24</sup>Y. Ueda, K. Kosuge, and S. Kachi, *Mater. Res. Bull.* **12**, 87 (1977).
- <sup>25</sup>S.A. Shivashankar and J.M. Honig, *Phys. Rev. B* **28**, 5695 (1983).
- <sup>26</sup>We have estimated  $\delta$  value, assuming excess oxygen ( $\text{LaTiO}_{3+y/2}$ ), but there is little difference ( $\Delta\delta\approx 0.01$ ) for the estimated value of  $\delta$  if we assume an La deficiency ( $\text{La}_{1-z}\text{TiO}_3$ ).
- <sup>27</sup>N. Môri, T. Nakanishi, M. Ohashi, N. Takeshita, H. Goto, S. Yomo, and Y. Okayama, *Physica B* (to be published).
- <sup>28</sup>V.J. Emery and S.A. Kivelson, *Phys. Rev. Lett.* **74**, 3253 (1995).
- <sup>29</sup>E. Abrahams and G. Kotliar, *Science* **274**, 1853 (1996), and references cited therein.
- <sup>30</sup>F.F. Assaad and M. Imada, *Phys. Rev. Lett.* **74**, 3868 (1995).
- <sup>31</sup>D.S. Marshall, D.S. Dessau, A.G. Loeser, C-H. Park, A.Y. Matsumura, J.N. Eckstein, I. Bozovic, P. Fournier, A. Kapitulnik, W.E. Spicer, and Z.-X. Shen, *Phys. Rev. Lett.* **76**, 4841 (1996).
- <sup>32</sup>H. Ding, T. Yokoya, J.C. Campuzano, T. Takahashi, M. Randeria, M.R. Norman, T. Mochiku, K. Kadowaki, and J. Giapintzakis, *Nature (London)* **382**, 51 (1996).
- <sup>33</sup>X.-G. Wen and P.A. Lee, *Phys. Rev. Lett.* **76**, 503 (1996); P.A. Lee, N. Nagaosa, T.-K. Ng, and X.-G. Wen, *Phys. Rev. B* **57**, 6003 (1998).
- <sup>34</sup>S. Miyasaka, H. Takagi, Y. Sekine, H. Takahashi, N. Môri, and R. J. Cava (unpublished).
- <sup>35</sup>S.A. Carter, T.F. Rosenbaum, P. Metcalf, J.M. Honig, and J. Spalek, *Phys. Rev. B* **48**, 16 841 (1993).
- <sup>36</sup>T. Yoshida, K. Kobayashi, T. Susaki, T. Mizokawa, A. Fujimori, Y. Taguchi, T. Katsufuji, and Y. Tokura (unpublished).
- <sup>37</sup>J.B. Sokoloff, *Phys. Rev.* **185**, 770 (1969).
- <sup>38</sup>Y. Murakami, H. Kawada, H. Kawata, M. Tanaka, T. Arima, Y. Moritomo, and Y. Tokura, *Phys. Rev. Lett.* **80**, 1932 (1998); Y. Murakami, J.P. Hill, D. Gibbs, M. Blume, I. Koyama, M. Tanaka, H. Kawata, T. Arima, Y. Tokura, K. Hirota, and Y. Endoh, *ibid.* **81**, 582 (1998).
- <sup>39</sup>T. Ishikawa, K. Ookura, and Y. Tokura, *Phys. Rev. B* (to be published 1 April 1999).
- <sup>40</sup>P. Kwisera, M.S. Dresselhaus, and D. Adler, *Phys. Rev. B* **21**, 2328 (1980).
- <sup>41</sup>Th. Pruschke, D.L. Cox, and M. Jarrell, *Phys. Rev. B* **47**, 3553 (1993).
- <sup>42</sup>T.M. Rice and W.F. Brinkman, *Phys. Rev. B* **5**, 4350 (1972).
- <sup>43</sup>C.M. Hurd, *The Hall Effect in Metals and Alloys* (Plenum Press, New York, 1972).
- <sup>44</sup>H. Fukuyama *J. Phys. Soc. Jpn.* **49**, 644 (1980).
- <sup>45</sup>B.L. Altshuler, D. Khmel'nitzkii, A.I. Larkin, and P.A. Lee, *Phys. Rev. B* **22**, 5142 (1980).
- <sup>46</sup>B. Shapiro and E. Abrahams, *Phys. Rev. B* **24**, 4025 (1981).
- <sup>47</sup>K. Ueda, *J. Phys. Soc. Jpn.* **43**, 1497 (1977).
- <sup>48</sup>T. Moriya, in *Spectroscopy of Mott Insulators and Correlated Metals*, edited by A. Fujimori and Y. Tokura (Springer, Berlin, 1995), pp. 66–79.
- <sup>49</sup>M. Kamada, N. Môri, and T. Mitsui, *J. Phys. C* **10**, L643 (1977).